Computers and Concrete, *Vol. 15*, *No. 6 (2015) 865-878*
DOI: http://dx.doi.org/10.12989/cac.2015.15.6.865

Multiscale modeling for compressive strength of concrete columns with circular cross-section

Han-liang Wu[1,2] and Yuan-feng Wang[*1]

[1]*School of Civil Engineering, Beijing Jiaotong University, Beijing, 100044, PR China*
[2] *Bridge Technology Research Center, Research Institute of Highway, Ministry of Transportation, Beijing, 100088, P R China*

(Received January 29, 2013, Revised January 1, 2015, Accepted January 15, 2015)

Abstract. In order to construct a multiscale model for the compressive strength of plain concrete columns with circular cross section subjected to central longitudinal compressive load, a column failure mechanism is proposed based on the theory of internal instability. Based on an energy analysis, the multiscale model is developed to describe the failure process and predict the column's compressive strength. Comparisons of the predicted results with experimental data show that the proposed multiscale model can accurately represent both the compressive strength of the concrete columns with circular cross section, and the effect of column size on its strength.

Keywords: multiscale modeling; analytical solution; energy analysis; fracture mechanics; circular concrete columns; size effect.

1. Introduction

The main aim of multiscale material science is to reveal the coupling relations between different spatial or temporal scales and the measured properties of the materials. It is recognized that multiscale science is rapidly becoming an essential part of computational science and engineering (Engquist *et al.* 2005). In material studies, one application of multiscale science is to predict the strength of heterogeneous materials (Cazacu 2008). In fact, the failure of most heterogeneous materials (like ceramic, rock and concrete) generally results from the internal microscopic damage, which means that the strength of heterogenous materials greatly depends on their micro-structure (Shackelford 2004). Therefore, understanding and modeling how the materials fail are of fundamental importance.

Concrete is a mixed material composed mainly of coarse aggregate, fine aggregate and cement mortar. It is a typical heterogeneous material which contains many initial microcracks after casting. These microcracks continue to grow and develop with the increase of external load, and then gradually form macrocracks which will lead to global failure of the concrete structures or members. Thus, the failure process of concrete exhibits micro-macro behavior on a spatial scale. Actually,

[*] Corresponding Author, Professor, E-mail: cyfwang@bjtu.edu.cn.
[a] Ph. D.
[b] Ph. D., Professor

http://www.techno-press.org/?journal=cac&subpage=8 ISSN: 1598-8198 (Print), 1598-818X (Online)

this micro-macro failure process is basically the same for any type of loading as long as the global failure is not caused by ductility (Bazănt and Planas 1998). During the micro-macro failure process, the micro-structure undergoes significant changes in which complex interactions play an important role. Therefore, an ideal failure model should include such interactions with multiscale modeling.

For concrete columns under axial compression, most researches in recent years have focused on numerical modeling, including some multiscale finite element modelings using new elements (e.g., lattice element (Grassl and Jirásek 2010, Grassl *et al.* 2012) and particle element (Qin and Zhang 2011, Lian *et al*. 2011)) or new constitutive models (e.g., microplane model (Bazănt and Caner 2005)). Howerver, analytical modeling for the columns is paid few attention, except the study of Bazănt and Xiang (1997). In their work, the compressive failure of concrete columns with rectangular cross section was modeled as damage propagation from a band of axial splitting microcracks inclined with the column axis. Based on the theory of internal instability (Bazănt and Cedolin 1991), the failure process was formulated as energy exchanges, and a simplified multiscale model for the compression failure of centrically or eccentrically loaded concrete columns was developed. Using their model, not only an analytical solution for the compression strength of columns was obtained, but also the size effect on the strength (i.e., the compressive strength decreases as the columns' size increases) was predicted. Although Bazănt and Xiang carried out a leading exploration in analytical multiscale modeling for concrete failure, their work had a main limitation: only columns with rectangular cross section were studied. However, columns with circular cross-section present a significantly different failure mode from rectangular cross-section columns (McCormac and Browm 2009). Thus, it will be hard for the model proposed by Bazănt and Xiang to be used in the analysis of the columns with circular cross-section, which are one of the most common practical applications of concrete columns, for example, bridge piers.

Based on the theory of internal instability, a failure mechanism is established for the centrally compressed plain concrete columns with circular cross section in the paper. A three-dimensional multiscale model, according this mechanism, is developed by the analysis of energy exchanges during the failure process under increasing axial loading. An analytical solution for the compressive strength of columns is deduced in term of an energy balance criterion of fracture mechanics. In addition, comparisons of experimental data with the results of the analytical model, together with an essential discussion of the results are presented.

2. Theory of internal instability

There are generally two kinds of failures that occur in concrete structures: strength failure and stability failure. Traditional strength failure studies generally do not account for geometrical characteristics such as shape, size, and slenderness. Stability failure, including overall and local instabilities, can be modeled according to a stability theory based only on the geometric characteristics of concrete structure. Thus, neither of the two theories alone can provide a complete solution for the common failure of concrete structures, since the strength failure and the stability failure modes exist simultaneously. Thus, Bazănt and Cedolin (1991) formulated a theory of internal instability that combined the strength and stability modes. Their formulation has been applied to a variety of heterogenous materials such as concrete (Bazănt and Xiang 1998), composites (Bazănt 1967), and rock (Bazănt *et al.* 1993).

The core ideas of the theory of internal instability are: 1) a macrocrack of concrete consists of a

band of concentrated parallel microcracks, which can divide the corresponding macro-structure into a mass of micro-structures; 2) global failure of concrete is triggered by instabilities of local micro-structures. Based on this theory, the failure process of compressed concrete can be described as follows (Bazănt and Xiang 1997): First, as the load increases, initial smeared microcracks continuously propagate and coalesce along the direction of principal compressive stress, and gradually become stacked to produce inclined compression-shear bands defined as en-echelon cracks, as shown in Figs. 1(a) and 1(b). Second, some micro-structures are generated by splits of the parallel en-echelon cracks, as shown in Fig. 1(b). Then the micro-structure suddenly looses its local stability, as shown in Fig. 1(c). Third, a macrocrack is formed at the locations of the disabled micro-structures, as shown in Fig. 1(d). Fig. 1 demonstrates the internal instability and damage development from the microscopic to the macroscopic scale, and an example of this multiscale modeling is the concrete failure (Bazănt and Xiang 1997).

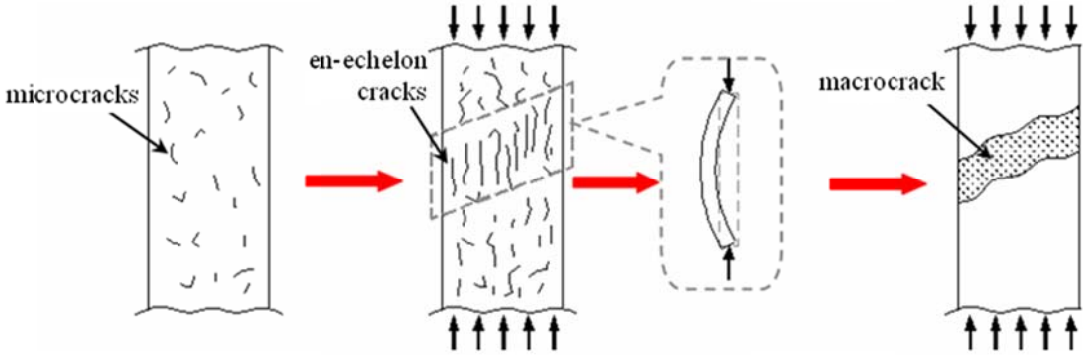

(a) Initial smeared microcracks

(b) Propagation and coalescence of microcracks, formation of en-echelon cracks

(c) Instability of micro-structures

(d) Formation of macrocrack

Fig. 1 Theory of internal instability

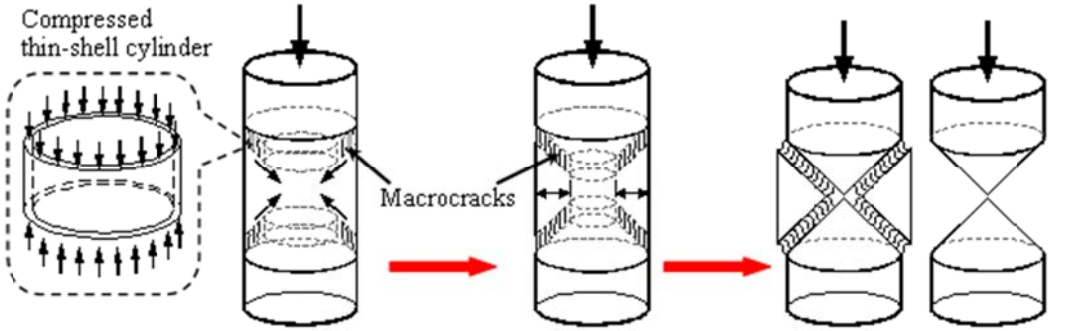

(a) Micro-structure

(b) Extension of macrocracks formation of en-echelon cracks

(c) Macrocracks reach critical length

(d) Formations of penetrating cross macrocracks and conical failure surfaces

Fig. 2 Failure mechanism of circular concrete columns subjected to central compressive load

3. Compressive failure mechanism of a circular concrete column

Based on the theory of internal instability, a failure mechanism of concrete columns with circular cross-section subjected to central compressive load is established herein. The mechanism, illustrated in Fig. 2, is based on the following four hypotheses.

Hypothesis I: At the moment of failure, the compressive load on the column as well as the axial deformation and the axial deformation remains unchanged. Concrete usually presents sudden and brittle failure, even explosive failure like that of high-strength concrete columns (ACI 1996) and fiber-reinforced concrete columns (Adepegba and Regan 1981). At the moment of failure, the extension of macrocracks is too fast to affect immediately the load and deformation of the columns. Therefore, the load (stress) and deformation (strain) are assumed to remain unchanged during the failure, except in the local regions close to the macrocracks.

Hypothesis II: The concrete column presents conical failure surfaces, which are determined by only one couple of penetrating cross macrocracks. As the compressive load increases, the microcracks increase in number and develop to macrocracks. All of the macrocracks will influence the final global failure of the column. However, there is only one couple of penetrating cross macrocracks that dominates the global failure, as shown in Figs. 2(b)-2(d).

Hypothesis III: The micro-structure is composed of microscopic thin-shelled cylinders subjected to compression, as shown in Fig. 2(a).

Hypothesis IV: The theory only applies to short, brittle failure concrete columns, while overall instability and ductility failure are not considered.

4. Energy analysis of compression failure of a concrete column with circular cross-section

4.1 Energy partition of a concrete column

Based on the theory of internal instability, a macrocrack is made of a group of en-echelon cracks. These groups are defined as crack band zones (CBZ, Bazănt and Oh 1983). After the macrocracks are formed, the stress in these zones close to the macrocracks decreases and there is a corresponding release of strain energy. These zones are defined as stress release zones (SRZ), depicted by the shaded regions in Fig. 3. Following the hypothesis I, there are no changes of the stress, strain and energy in the zones outside of the CRZ and SRZ. Those outside zones are defined as rigid body zones (RBZ). Therefore, the concrete column with circular cross-section is divided into three parts, each with different changes in energy, as shown in Fig. 3. Here m is the width of CBZ, which is also the height of microscopic thin-shelled cylinders; d is the diameter of the column; h is the height of the column; θ is the inclined angle of macrocracks; s is the distance between adjacent en-echelon cracks, which is the thickness of microscopic thin-shelled cylinders; a is the critical length of macrocrack; k is the slope of boundary lines of the SRZ; and r is the radial coordinate.

At the moment of the global failure is reached, the strain in a concrete column is εf, and the stress is σ_f, which is equal to the column's compressive strength. During the failure process, the stresses and strains in the CRZ and SRZ change, as do their energies.

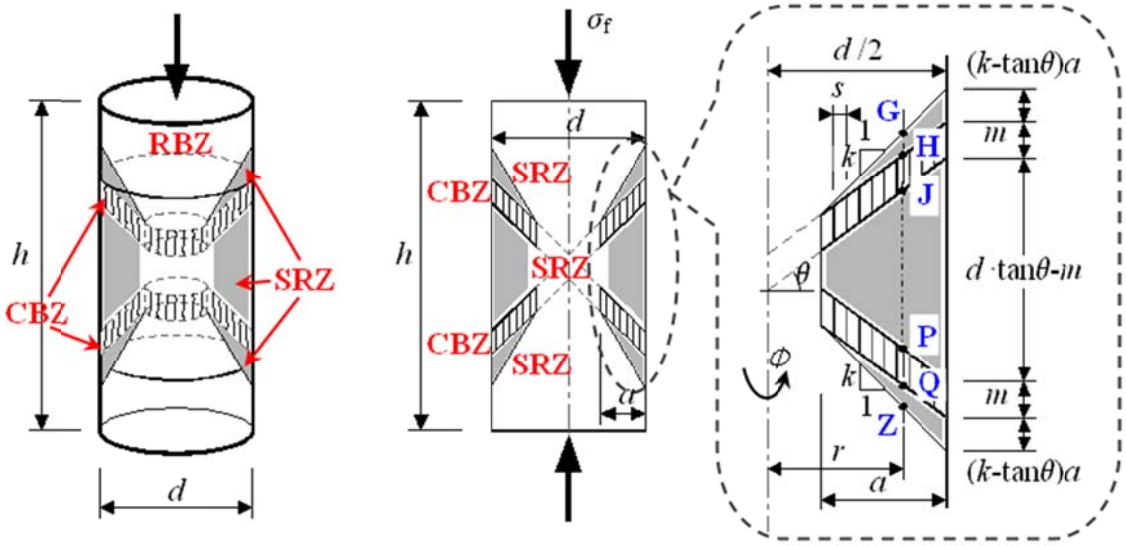

(a) Circular concrete column (b) Longitudinal-section of the column

Fig. 3 Energy partition of circular concrete column

4.2 Energy analysis of the SRZ

When the microscopic thin-shelled cylinders in the CBZ loss their stability, the stress in the SRZ is reduced to an instability stress (σ_{cr}). Considered the linear elastic unloading process shown in Fig. 41(a), the decrease of strain energy density in the SRZ ($\Delta\overline{\Pi}_{SRZ}$) is equal to the shaded areas shown in Fig. 4(a), or

$$\Delta\overline{\Pi}_{SRZ} = \frac{\sigma_{cr}^{\ 2}}{2E_{c0}} - \frac{\sigma_f^{\ 2}}{2E_{c0}} \tag{1}$$

The total release of strain energy in the SRZ ($\Delta\Pi_{SRZ}$) is obtained by integration as follow

$$\begin{aligned}\Delta\Pi_{SRZ} &= \int \Delta\overline{\Pi}_{SRZ}\, \mathrm{d}V_{SRZ} \\ &= \int_{d/2-a}^{d/2}\int_0^{2\pi}\left\{\frac{\left(\sigma_{cr}^{\ 2}-\sigma_f^{\ 2}\right)}{2E_{c0}}\cdot\left[2(k-\tan\theta)(r-\frac{d}{2}+a)+(2r\tan\theta-m)\right]\right\} r\mathrm{d}\phi\mathrm{d}r\end{aligned} \tag{2}$$

where ϕ is the rotation angle around the axis of columns; E_{c0} is the elastic modulus of concrete; and V_{SRZ} is the volume of the SRZ.

4.3 Energy analysis of the CBZ

The instability of the microscopic thin-shelled cylinders results in a nonlinear unloading process in the CBZ. The unloading process ends with a residual stress σ_{cr} and a residual strain ε_c, as shown in Fig. 4(b). The strain in the CBZ can be determined from the compatibility condition of

hypothesis I. That is, since the RBZ behaves as a rigid body during the failure process, the boundary lines between the RBZ and SRZ are fixed. It means that the deformation of line segment **GZ** at any r does not change during the failure process, as shown in Fig. 3(b). The result is the following equation

$$\left[2(k-\tan\theta)(r-\frac{d}{2}+a)+(2r\tan\theta-m)\right]\cdot\left(\varepsilon_{\mathrm{cr}}-\varepsilon_{\mathrm{f}}\right)+2m\cdot\left(\varepsilon_{\mathrm{c}}-\varepsilon_{\mathrm{f}}\right)=0 \tag{3}$$

which can be rewritten as

$$\begin{aligned}\varepsilon_{\mathrm{c}} &= \varepsilon_{\mathrm{f}}+\frac{2(k-\tan\theta)(r-\frac{d}{2}+a)+(2r\tan\theta-m)}{2m}\cdot\left(\varepsilon_{\mathrm{f}}-\varepsilon_{\mathrm{cr}}\right)\\ &= \varepsilon_{\mathrm{f}}+\frac{2(k-\tan\theta)(r-\frac{d}{2}+a)+(2r\tan\theta-m)}{2m}\cdot\frac{\left(\sigma_{\mathrm{f}}-\sigma_{\mathrm{cr}}\right)}{E_{\mathrm{c0}}}\end{aligned} \tag{4}$$

The decrease of strain energy density in the CBZ ($\Delta\overline{\Pi}_{\mathrm{CBZ}}$) is

$$\Delta\overline{\Pi}_{\mathrm{CBZ}}=-\frac{\left(\sigma_{\mathrm{cr}}-\sigma_{\mathrm{f}}\right)^2}{2E_{\mathrm{c0}}}+\sigma_{\mathrm{cr}}\cdot\left(\varepsilon_{\mathrm{c}}-\varepsilon_{\mathrm{f}}\right) \tag{5}$$

The total release of strain energy in the CBZ ($\Delta\Pi_{\mathrm{CBZ}}$) is obtained by integration

$$\begin{aligned}\Delta\Pi_{\mathrm{CBZ}} &= \int\Delta\overline{\Pi}_{\mathrm{CBZ}}\,\mathrm{d}V_{\mathrm{CBZ}}\\ &= \int_{d/2-a}^{d/2}\int_0^{2\pi}\left\{-\frac{\left(\sigma_{\mathrm{cr}}-\sigma_{\mathrm{f}}\right)^2}{2E_{\mathrm{c0}}}+\sigma_{\mathrm{cr}}\cdot\frac{\left(\sigma_{\mathrm{f}}-\sigma_{\mathrm{cr}}\right)}{E_{\mathrm{c0}}}\right.\\ &\left.\cdot\frac{2(k-\tan\theta)(r-d/2+a)+(2r\tan\theta-m)}{2m}\right\}\cdot 2m\cdot r\,\mathrm{d}\phi\,\mathrm{d}r\end{aligned} \tag{6}$$

(a) Unloading path in SRZ (b) Unloading path in CBZ

Fig. 4 Unloading path of energy relief zones

where V_{CBZ} is the volume of the CBZ. The total release of strain energy during the failure process ($\Delta\Pi$) is the sum of the energy releases in the SRZ and the CBZ. That is

$$\Delta\prod = \Delta\prod_{SRZ} + \Delta\prod_{CBZ}$$
$$= \int_{d/2\text{-}a}^{d/2}\int_{0}^{2\pi}\left\{-\frac{\left(\sigma_{cr}-\sigma_{f}\right)^{2}}{2E_{c0}}\cdot\left[2(k-\tan\theta)(r-\frac{d}{2}+a)+(2r\tan\theta-m)\right]\right.$$
$$\left.-\frac{\left(\sigma_{cr}-\sigma_{f}\right)^{2}}{2E_{c0}}\cdot 2m\right\} r\mathrm{d}\phi\mathrm{d}r \tag{7}$$

4.4 Analytical solution for compressive strength of a column

Based on the energy balance criterion of fracture mechanics (Anderson 2005), when the length of macrocrack reaches its critical value, which is also named as the critical crack length, the energy release rate must be equal to the rate at which the energy is consumed by formation of macrocrack. That is

$$-\frac{\partial(\Delta\prod)}{\partial\ A_{f}} = G_{f} \tag{8}$$

where G_f is the energy release rate of concrete, G_f=(0.005~0.01)·f_t, here f_t is the tensile strength of concrete (Hillerborg *et al*. 1983); and A_f is the fracture area of macrocrack, which is equal to the total area of en-echelon cracks. From Fig. 3, that area is

$$A_{f} = 2\sum_{n=0}^{a/s-1}\left[2\pi\cdot m\cdot(\frac{d}{2}-a+s\cdot n)\right] = 4\pi\cdot m\cdot\left[(\frac{d}{2}-a)\cdot\frac{a}{s}+s\cdot\frac{1}{2}\cdot(\frac{a}{s}-1)\cdot\frac{a}{s}\right] \tag{9}$$

The distance between adjacent en-echelon microcracks is so small that the value of a/s is much greater than one. Thus, Eq. (10) can be simplified to give

$$A_{f} \approx 4\pi\cdot m\cdot\left[(\frac{d}{2}-a)\cdot\frac{a}{s}+s\cdot\frac{1}{2}\cdot\frac{a}{s}\cdot\frac{a}{s}\right] = 2\pi\cdot m\cdot\left[\frac{d\cdot a}{s}-\frac{a^{2}}{s}\right] \tag{10}$$

The energy balance criterion can be written as

$$-\frac{\partial(\Delta\prod)}{\partial\ A_{f}} = -\frac{\partial(\Delta\prod)/\partial a}{\partial\ A_{f}/\partial a}$$
$$= \frac{\pi\cdot\frac{\left(\sigma_{cr}-\sigma_{f}\right)^{2}}{2E_{c0}}\cdot\left[(3\tan\theta-k)\cdot\left(\frac{d}{2}-a\right)^{2}+(k-\tan\theta)\left(\frac{d}{2}\right)^{2}+m\cdot\left(\frac{d}{2}-a\right)\right]}{2\pi\cdot m\cdot\left(\frac{d}{s}-\frac{2a}{s}\right)} = G_{f} \tag{11}$$

It follows that the stress results are

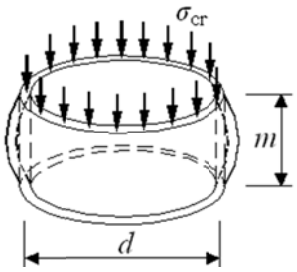

Fig. 5 Instability modes of microscopic thin-shelled cylinders

$$(\sigma_{cr}-\sigma_f)^2=\frac{2G_f\cdot m\cdot E_{c0}\cdot\left(\frac{d}{s}-\frac{2a}{s}\right)}{\left[(3\tan\theta-k)\cdot\left(\frac{d}{2}-a\right)^2+(k-\tan\theta)\cdot\left(\frac{d}{2}\right)^2+m\cdot\left(\frac{d}{2}-a\right)\right]} \tag{12}$$

Since $\sigma_f \geq \sigma_{cr}$, the compressive strength becomes

$$\sigma_f=\sigma_{cr}+\left\{\frac{2G_f\cdot m\cdot E_{c0}\cdot(d/s-2a/s)}{\left[(3\tan\theta-k)\cdot(d/2-a)^2+(k-\tan\theta)\cdot(d/2)^2+m\cdot(d/2-a)\right]}\right\}^{\frac{1}{2}} \tag{13}$$

4.5 Instability stress of a microscopic thin-shelled cylinder

At a certain moment of loading, the microscopic thin-shelled cylinder looses its stability under compressive load, as shown in Fig. 5. The instability stress is calculated (Samuelson and Eggwertz 1992) as

$$\sigma_{cr}=\frac{\pi^2E_{c0}}{12(1-\nu^2)}\cdot\frac{s^2}{m^2}+\frac{4E_{c0}}{\pi^2}\cdot\frac{m^2}{d^2} \tag{14}$$

where v is the Poisson's ratio of concrete.

4.6 Determination of the parameters in the solution

To aid in the evaluation of σ_f, Eq. (13), five parameters (m, a, θ, k and s) are identified. Of these, m is related to the composition of concrete, such as the size and shape of aggregates, and the strength of cement. The ratio of a/d is assumed to be a constant when the columns have the similar geometric characteristics, such as the shape of the cross section, the height-to-width ratio; and the failure modes such as the angle of the macrocracks. Both m and a/d can be determined by experiment (Bazănt and Xiang 1997).

The value of k can be determined by experiment or by solving the elastic stress field (Bazănt and Xiang 1997). In this study, a finite element analysis (FEA) was applied in the longitudinal-section of columns with macrocracks, as shown in Fig. 3(b). Shown in Fig. (6) are the

results of FEA. It is observed that the boundary edges of the SRZ are significantly influenced by the value θ but not by a/d. Based on the results, a regression formula of k is proposed to keep same size SRZ. That is, the area surrounded by the boundary edges from FEA and the macrocrack is numerically equal to that surrounded by the straight-line with slope of k and the macrocrack, as shown in Fig. (6). The result is

$$k = 1 + 0.52 \cdot \tan\theta \tag{15}$$

Similar to the solution of other heterogenous materials (Bazănt *et al.* 1993), based on the second law of thermodynamics, the value of s can be determined so that σ_f is minimized. The necessary condition of minimum is

$$\frac{\partial\, \sigma_f}{\partial\, s} = 0 \tag{16}$$

Substituting Eqs. (13) and (14) into Eq. (16), this minimum is obtained

$$\frac{\pi^2 E_{c0}}{12(1-\nu^2)} \cdot \frac{2s}{m^2} = \frac{1}{2} s^{-\frac{3}{2}} \cdot \left\{ \frac{8G_f \cdot m \cdot E_{c0} \cdot (d-2a)}{\left[(3\tan\theta - k) \cdot (d-2a)^2 + (k - \tan\theta) \cdot d^2 + 2m \cdot (d-2a) \right]} \right\}^{\frac{1}{2}} \tag{17}$$

The value of s is calculated from

$$s = \left[\frac{72}{\pi^4} \right]^{\frac{1}{5}} \cdot m \cdot \left\{ \frac{G_f \cdot (d-2a) \cdot (1-\nu^2)^2}{E_{c0} \left[(3\tan\theta - k) \cdot (d-2a)^2 + (k - \tan\theta) \cdot d^2 + 2m \cdot (d-2a) \right]} \right\}^{\frac{1}{5}} \tag{18}$$

From the Eqs. (15) and (18), the analytical solution for compressive strength of circular concrete columns is computed as

$$\sigma_f = 3.643 \left[\frac{G_f^{\,2} \cdot E_{c0}^{\,3} \cdot (d-2a)^2}{[(2.48\tan\theta - 1) \cdot (d-2a)^2 + (1 - 0.48\tan\theta) \cdot d^2 + 2m \cdot (d-2a)]^2 \cdot (1-\nu^2)} \right]^{\frac{1}{5}} + \frac{4E_{c0}}{\pi^2} \cdot \frac{m^2}{d^2} \tag{19}$$

5. Size effect on compressive strength of the columns

This analytical solution can be written simply as

$$\sigma_f = \frac{C_1}{(C_2 \cdot d + C_3)^{\frac{2}{5}}} + \frac{C_4}{d^2} \tag{20}$$

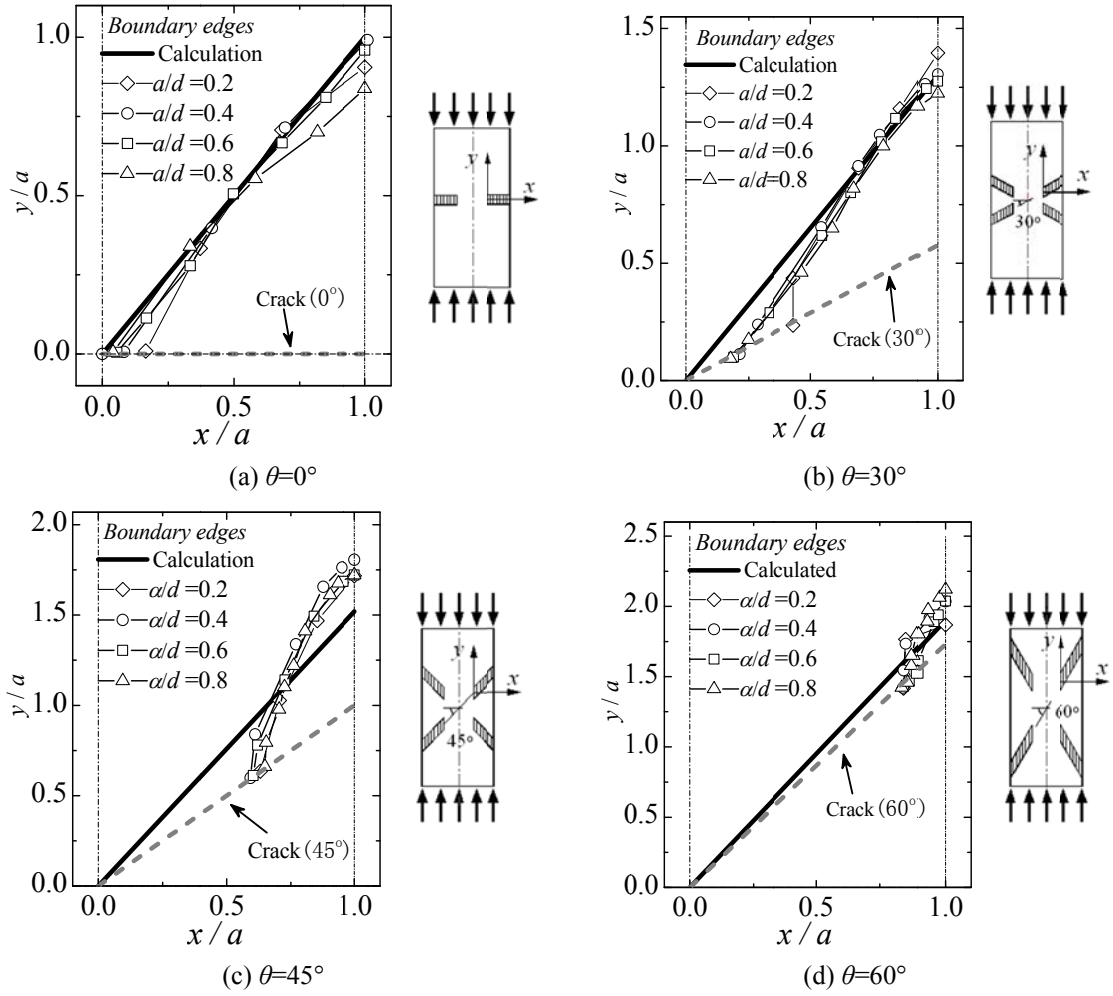

Fig. 6 Boundary edges of SRZ from FEA and calculation

in which C_1, C_2, C_3, and C_4 are synthesis parameters, calculated as follows

$$C_1 = \left[\frac{3.643 \cdot G_f^{\,2} \cdot E_{c0}^{\,3} \cdot (1-2\lambda)^2}{(1-\nu^2)} \right]^{\frac{1}{5}} \tag{21}$$

$$C_2 = (2.48\tan\theta - 1) \cdot (1-2\lambda)^2 + (1 - 0.48\tan\theta) \tag{22}$$

$$C_3 = 2m \cdot (1-2\lambda) \tag{23}$$

$$C_4 = \frac{4E_{c0} \cdot m^2}{\pi^2} \tag{24}$$

where $\lambda = a/d$.

Thus, this proposed solution is a function of column size, which means that the solution can exhibit the size effect on compressive strength of the concrete columns with circular cross-section subjected to a central compressive load. Furthermore, from Eq. (20), one observes that the ratio of $\log(\sigma_f)/\log(d)$ is a certain value between -1/2 and -2/5, which is within the accepted range of size effect of concrete (-1/2 to 0, Bazănt and Planas 1998).

6. Comparisons with experimental data

We tested 18 reduced-scale concrete columns at Beijing Jiaotong University. All of these columns were of circular cross section, and they were divided into two groups based on different concrete strength (f_{c0}). Three different sizes for each group were used, where d×h=70×210, 105×315, and 194×582 mm for the small, medium, and large columns, respectively. The grade of concrete strength herein was 28.79 and 50.64 MPa, and the maximum aggregate size was 20 mm. In addition, 60 sets of experimental data reported by other researchers (Samuelson and Eggwertz 1992, Şener 1997) were also used herein. Shown in Table 1 are the details of all of these experimental data.

Comparisons of the experimental data with the predictions from our multiscale model are shown in Fig. 7. Here, the points show the experimental data and the solid lines show the analytical solutions. The value of θ is fixed as 45^o and the parameters λ and m are identified by the regression of experimental data. It is observed that our model represents the experimental data quite well, especially for the reduced-scale concrete columns with circular cross-section. However, the deviations of the model from the experimental data of small specimens are relatively large. A reason for this is that the concrete columns of diminished size exhibit plastic and ductile compressive failure modes (Bazănt and Planas 1998), which are conditions beyond the range of

Table 1 Details of experimental data

Group No.	Researchers	f_{c0} (MPa)	Size (d×h, mm)	Measured strength (MPa)
A	the authors	50.64	70×210	52.0, 41.1, 40.9
			105×315	39.2, 34.4, 32.3
			194×582	34.3, 41.0, 36.6
B	the authors	28.79	70×210	24.0, 23.5, 23.0
			105×315	22.8, 22.7, 23.2
			194×582	19.8, 19.4, 18.6
C	Yi. *et al.* (2006)	45.68	50×100	50.4, 52.5, 44.2, 45.8, 43.1, 47.2
			100×200	48.1, 45.5, 43.9, 45.2
			150×300	44.2, 40.4, 44.2
			200×400	43.7, 46.5
D	Yi. *et al.* (2006)	66.00	50×100	69.4, 71.1, 74.0, 74.8, 72.9, 74.9
			100×200	67.5, 66.6, 65.5, 64.4
			150×300	62.7, 66.3, 68.8
			200×400	64.4, 66.5
E	Yi. *et al.* (2006)	80.10	50×100	97.8, 91.5, 92.5, 92.4, 83.4
			100×200	75.9, 79.9, 80.6, 64
			150×300	80.1, 76.1
			200×400	71.3
F	Şener. (1997)	37.74	37.5×70	48.0, 47.1, 44.4, 39.8, 45.3
			75×150	31.5, 35.3, 38.0, 41.6, 42.3
			150×300	34.0, 34.0, 37.3, 35.7, 40.9

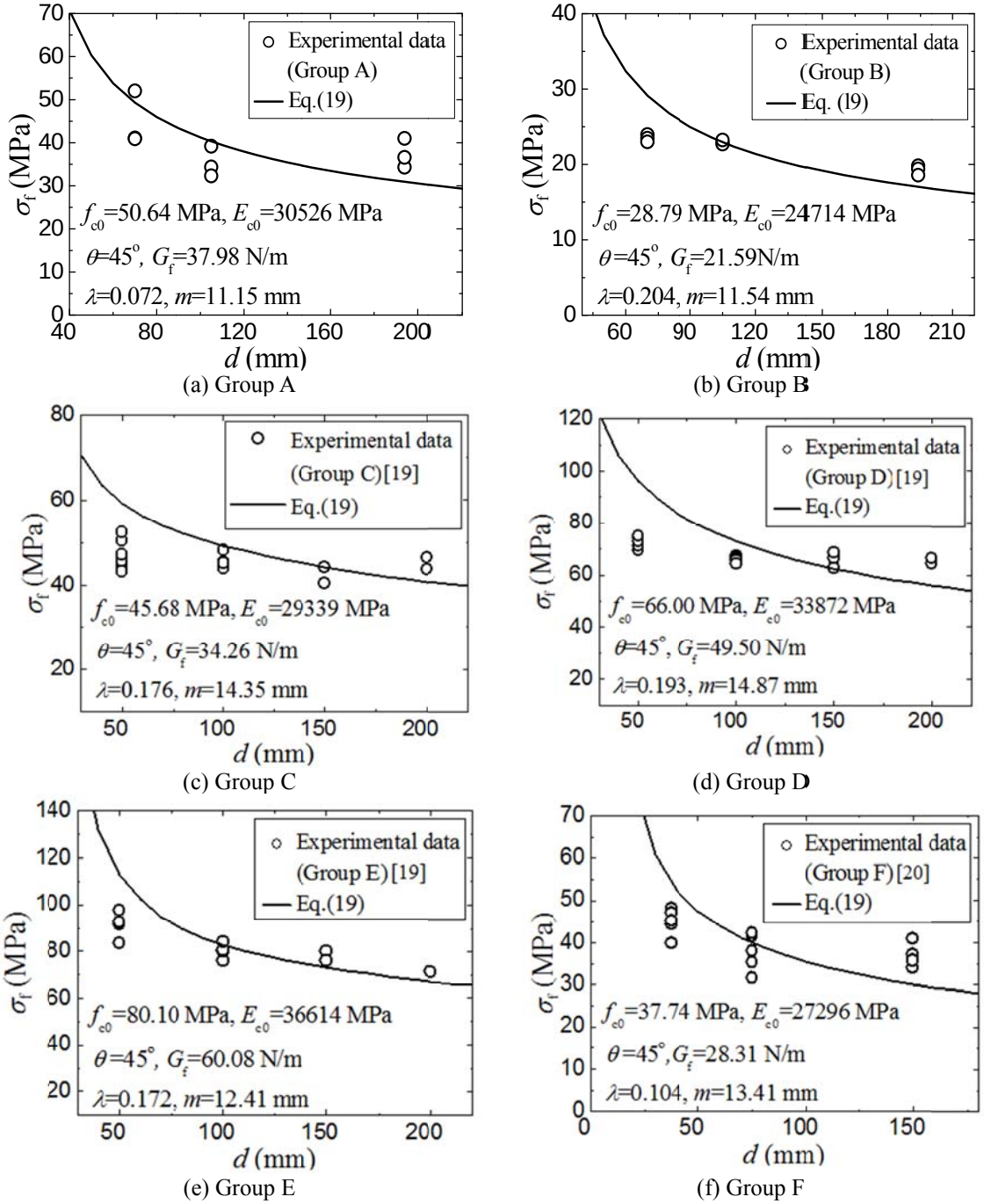

Fig. 7 Comparison of the proposed model with experimental data

the theory of internal instability. However, it is also observed in Fig. 7 that the size effect on compressive strength of the columns is predicted quite well: that the compressive strength of the

columns decreases as the size increases.

7. Conclusions

A multiscale model for predicting the compressive strength of concrete columns with circular cross-section under central compressive load was successfully developed herein. Comparison of the predicted results with experimental data and some discussions are included. The following conclusions are drawn from the study.

- Based on the theory of internal instability, a rational brittle failure mechanism is established. The mechanism represents a micro-macro failure process, a damage propagation of compressive failure. In this mechanism, the compressive failure process of the concrete columns with circular cross-section is divided into three steps, i.e., the formation of en-echelon cracks, the instability of microscopic thin-shelled cylinders, and the global failure of columns.
- An energy analysis is used to describe the failure process. An analytical solution for the compressive strength of the columns is deduced using an energy balance criterion of fracture mechanics. In the solution, three free parameters are identified by experiment and the size of columns is also included, which means that the solution can exhibit the size effect on the compressive strength of circular concrete columns. The logarithmic ratio of the compressive strength to size is a certain value between -1/2 and -2/5, which is within the accepted range of size effect of concrete.
- Comparisons with the experimental data demonstrate that the proposed multiscale model results agree well with the experimental data and predicts successfully the size effect on the compressive strength of the concrete columns with circular cross-section.

References

Adepegba, D. and Regan, P.E. (1981), "Performance of steel fibre reinforced concrete in axial loaded short columns", *Int. J. Cem. Compos. Lightweigh Concr.*, **3**(4), 255-259.

American Concrete Institute (ACI), (1996), *High-strength concrete columns: state of the art*, Reported by Joint ACI-ASCE Committee 441, Detroit.

Anderson, T. L. (2005), *Fracture Mechanics*, Oxon, Taylor & Francis.

Bazănt, Z.P. (1967), *Stability of continuum and compression strength*, Bulletin, RILEM.

Bazănt, Z.P. and Caner, F.C. (2005), "Microplane model M5 with kinematic and static constraints for concrete fracture and anelasticity I: Theory", *J. Eng. Mech.*, **131**(1), 31-40.

Bazănt, Z.P. and Cedolin, L. (1991), *Stability of Structures: Elastic, Inelastic, Fracture and Damage Theories*, New York, Oxford University Press.

Bazănt, Z.P., Lin, F. and Lippmann, H. (1993), "Fracture energy release and size effect in borehole breakout", *Int. J. Num. Anal. Meth. Geomech.*, **17**(1), 1-14.

Bazănt, Z.P. and Oh, B.H. (1983), "Crack band theory for fracture of concrete", *Mater. Struct.*, **16**(3), 155-177.

Bazănt, Z.P. and Planas, J. (1998), *Fracture and Size Effect in Concrete and Other Quasibrittle Materials*, Boca Roton, CRC Press.

Bazănt, Z.P. and Xiang, Y. (1997), "Size effect in compression fracture: splitting crack band propagation", *J. Eng. Mech*., **123**(2), 162-172.

Cazacu, O. (2008), *Multiscale Modeling of Heterogeneous Materials*, NewJersey, John Wiley & Sons Inc.
Engquist, B., Lötstedt, P. and Runborg, O. (2005), *Multiscale Methods in Science and Engineering*, Netherlands, Springer.
Grassl, P., Gregoire, D., Solano, L.R. and Cabot, G.P. (2012), "Meso-scale modeling of the size effect on the fracture process zone of concrerte", *Int. J. Solids Strct.*, **49**(13), 1818-1827.
Grassl, P. and Jirásek, M. (2010), "Meso-scale approach to modeling the fracture process zone of concrete subjected to uniaxial tension", *Int., J. Solids. Struct.*, **47**(7), 957-968
Hillerborg, A., Modéer, M. and Petersson, P.E. (1976), "Analysis of crack formation and crack growth in concrete by means of fracture mechanics and finite elements", *Cem. Concr. Res*., **6**(6), 773-782.
Lian, Y.P., Zhang, X., Zhou, X. and Ma, Z.T. (2011), "A FEMP method and its application in modeling dynamic response of reinforced concrete subjected to impact loading", *Comput. Method. Appl. Mech. Eng.*, **200**(17-20), 1659-1670.
McCormac, J.C. and Browm, R.H. (2009), *Design of reinforced concrete*, NewJersey, John Wiley & Sons.
Qin, C. and Zhang, C. (2011), "Numerical study of dynamic behavior of concrete by meso-scale particle element modeling", *Int. J. Impact Eng.*, **38**(12), 1011-1021.
Samuelson, L.A. and Eggwertz, S. (1992), *Shell Stability Handbook*, Oxon, Taylor & Francis.
Şener, S. (1997), "Size effect tests of high strength concrete", *J. Mater. Civil. Eng.*, **9**(1), 46-48.
Shackelford, F. (2004), *Introduction to Material Science for Engineers*, New York, Prentice Hall.
Yi, S., Yang, E. and Choi, J. (2006), "Effect of specimen sizes, specimen shapes, and placement directions on compressive strength of concrete, *Nucl. Eng. Des.*, **236**(2), 115-127.

CC